

# Probing the electron density in undoped, Si-doped, and Mg-doped InN nanowires by means of Raman scattering

R. Cuscó,<sup>1</sup> N. Domènech-Amador,<sup>1</sup> L. Artús,<sup>1,a)</sup> T. Gotschke,<sup>2,3</sup> K. Jeganathan,<sup>2,4</sup>  
T. Stoica,<sup>2</sup> and R. Calarco<sup>2,3</sup>

<sup>1</sup>*Institut Jaume Almera, Consell Superior d'Investigacions Científiques (CSIC), Lluís Solé i Sabarís s.n., 08028 Barcelona, Spain*

<sup>2</sup>*Institute of Bio- and Nanosystems, Research Center Jülich GmbH, 52425 Jülich, Germany*

<sup>3</sup>*Paul-Drude-Institut für Festkörperelektronik, Hausvogteiplatz 5-7, 10117 Berlin, Germany*

<sup>4</sup>*Center for Nanoscience and Nanotechnology, Bharathidasan University, Tiruchirappalli 620024, India*

(Received 14 October 2010; accepted 5 November 2010; published online 30 November 2010)

We report a Raman scattering determination of the electron density in InN nanowires from the analysis of longitudinal optical-phonon-plasmon coupled modes. A Raman peak assigned to the  $L^-$  coupled mode is observed in both undoped and doped InN nanowires. This peak exhibits a shift to higher (lower) frequencies in the Si-doped (Mg-doped) nanowires and allows us to estimate the electron density in the nanowires. A significant residual electron density is found in the undoped nanowires, which increases in Si-doped nanowires and is partially compensated in Mg-doped nanowires. © 2010 American Institute of Physics. [doi:10.1063/1.3520643]

InN has received much attention as a promising material for optoelectronic devices and ultrafast electronics owing to its unique properties (narrow bandgap, small electron effective mass, high electron mobility, and drift velocity). The direct bandgap of InN can be increased by Ga alloying to cover a wide spectral range (0.7–3.4 eV). This makes InGaN the choice material system for light emitting devices from blue to red.<sup>1</sup> However, because of the lack of a suitable lattice matched substrate, a high density of threading dislocations and residual electrons is generally present in epitaxial layers. This drawback can be partly overcome by the self-assembled growth of InN nanocolumns, in which the lateral strain relaxation makes it possible to obtain nearly defect-free single crystalline nanowires.<sup>2</sup> Recently, the growth of nearly defect-free, nontapered InN nanowires with residual doping  $\leq 10^{16}$  cm<sup>-3</sup> and negligible accumulation at the lateral nonpolar faces has been reported.<sup>3</sup> The increased crystal quality and the possibility of tuning the emission energy of InGaN quantum wires make these structures very attractive for solid state lighting and next generation solar cells.<sup>4</sup>

InN is known to exhibit a large electron accumulation at the surface, giving rise to strong electric fields and quantized electron levels in a surface layer of a few nanometers.<sup>5</sup> Even for nonpolar surfaces ( $m$ -plane and  $a$ -plane) electron accumulation is predicted in the case of metal-rich surface reconstruction.<sup>6</sup> Such high conductive surface layer dominates the electrical transport properties of InN nanowires and obscures the electrical characterization of volume charge inside the nanowires. In contrast, Raman scattering by longitudinal optical (LO) phonon-plasmon coupled modes (LOPCMs) can provide a contactless probe into the volume electron density of the InN nanowires. As discussed in previous works on epitaxial InN layers,<sup>7,8</sup> the electrons in the quantized levels of the accumulation layer cannot sustain longitudinal plasma excitations, and therefore LOPCMs originate in the bulk InN.

In this letter, we present Raman scattering experiments on undoped Si- and Mg-doped InN nanowires in which the

low-frequency coupled mode  $L^-$  is detected. The  $L^-$  peak shows a frequency shift in Si- and Mg-doped samples relative to the undoped ones and it allows us to determine the volume electron density in the InN nanowires.

The nanowires were grown catalyst-free by plasma assisted molecular beam epitaxy under N-rich conditions on Si(111) substrates. The undoped wires (sample S0) have a diameter between 30 and 110 nm and a length up to 1  $\mu$ m. Nominally  $n$ -doped wires (samples S1–S3) were grown by supplying a Si flux with a beam equivalent pressure between 3 and  $5.8 \times 10^{-8}$  mbar. Nanowires with diameters between 60 and 180 nm and lengths up to 2.5  $\mu$ m were obtained. Nominally  $p$ -doped wires (samples M1 and M2) were grown with Mg fluxes of 1 and  $3 \times 10^{-9}$  mbar. The nanowires are single crystalline with the  $c$  axis parallel to the wire but with some point defects and stacking faults more frequently at the base of the wires. All samples exhibit a small tilt of the wire axis relative to the surface normal of the substrate. Details of the growth mechanism have been discussed elsewhere.<sup>9</sup>

Visible and ultraviolet (UV) Raman spectra of the as grown wires were obtained in near-backscattering geometry using 514.5 and 325 nm wavelength excitation. The scattered light was analyzed using a Jobin Yvon T64000 spectrometer with conventional macrocamera optics, which in contrast with single wire measurements<sup>10</sup> ensures a low power density and an average measurement over a large number of nanowires.

The as grown nanowires display a very large lateral-to-top surface ratio, and therefore most of the excitation light enters the nanowires through lateral faces. Taking into account the geometry of the experiment and the high refractive index of InN, the propagation direction of the light is then close to perpendicular to the  $c$  axis. The scattered light is collected (i) through the lateral faces in  $x(\cdot\cdot)\bar{x}$ -like backscattering configuration, where  $E_2$ ,  $A_1(\text{TO})$ , and  $E_1(\text{TO})$  modes are allowed, (ii) through a different lateral facet in near-in-plane, off-backscattering geometry where the  $E_1$  (LO) mode is also dipole allowed, or (iii) guided along the wire axis in  $x(\cdot\cdot)z$ -like scattering configuration, in which case only the  $E_2$  symmetry is allowed. Because of the scattering geometry, the quasi-LO modes observed in the

<sup>a)</sup>Electronic mail: lartus@ija.csic.es.

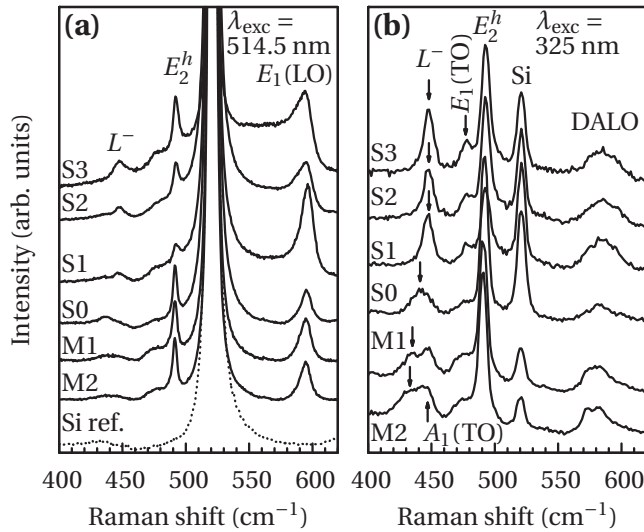


FIG. 1. Raman spectra of undoped (S0), silicon doped (S1–S3), and magnesium doped (M1, M2) InN nanowires obtained using (a) visible and (b) ultraviolet excitation.

experiment<sup>11</sup> contain a strong  $E_1$  (LO) component and will hereafter be generically referred to as  $E_1$  (LO) modes.

Raman spectra of the undoped and doped wires are shown in Fig. 1. A strong signal from the Si substrate is present in the visible Raman spectra [Fig. 1(a)]. For comparison purposes, the Raman spectrum of Si is also displayed (dotted line). The spectra of the nanowire samples show two main Raman peaks at 491 and 595  $\text{cm}^{-1}$ , corresponding to the  $E_2^{\text{high}}$  and  $E_1$  (LO) modes, respectively. Two weaker features can be observed at 475  $\text{cm}^{-1}$ , corresponding to the  $E_1$  (TO) mode, and in the 430–450  $\text{cm}^{-1}$  frequency range. The latter can hardly be discerned in samples M1 and M2 from the weak second-order band of the Si spectrum, but in the undoped and Si-doped samples it becomes sharper and appears to shift to higher frequencies. Such a shift cannot be attributed to strain in the nanowires, since they are mostly relaxed as indicated by the constant frequency of the  $E_2^{\text{high}}$  mode (see Fig. 2). Then, we assign these weak shifting modes to the  $L^-$  branch of  $E_1$  (LO)-phonon-plasmon coupled modes. Similar to the case of InN epilayers,<sup>7</sup> the high frequency branch ( $L^+$ ) could not be detected in our experiments. The intensity ratio between the LO and the  $E_2^{\text{high}}$  peaks is about four times higher in the nanowires as compared to the InN epilayers<sup>7</sup> as a consequence of their much higher surface to volume ratio. Given that the observation of the unscreened LO modes can be attributed to an electric-field induced resonant scattering mechanism in the accumulation layer,<sup>7</sup> and that such accumulation layer is usually present in the lateral nonpolar faces,<sup>12</sup> the scattering volume for the uncoupled LO modes is significantly enhanced in nanowires.

To unambiguously discern the  $L^-$  Raman peak from the Si substrate signal, Raman scattering measurements were performed in the UV region. Because of the strong optical absorption, the UV Raman spectra displayed in Fig. 1(b) show a dramatic reduction of the Si substrate signal and distinctly reveal the InN spectra of the nanowires. Here, the  $L^-$  peaks are clearly observed even in the Mg-doped samples, where they have shifted to lower frequencies and the  $A_1$  (TO) mode at 447  $\text{cm}^{-1}$  is resolved. It is interesting to note that the  $L^-$  peak is broader in the undoped sample S0 and sharpens up in Si-doped samples S1–S3, as expected for an  $L^-$

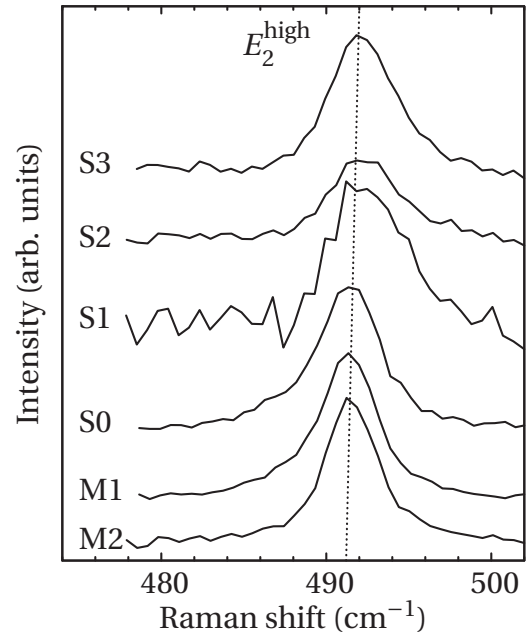


FIG. 2. Raman spectra of the  $E_2^{\text{high}}$  mode for undoped (S0), silicon doped (S1–S3), and magnesium doped (M1, M2) InN nanowires obtained using visible excitation after subtraction of the Si background.

coupled mode that gains phononlike character with increasing carrier density.

We notice a striking difference in the UV spectra in relation to the visible spectra regarding the LO mode intensity. The strong  $E_1$  (LO) peak that was observed in the visible spectra is totally absent of the UV spectra, where only a weak, disorder-activated longitudinal-optical (DALO) broad band centered at about 580  $\text{cm}^{-1}$  which reflects the phonon density of states can be seen. We have observed the same effect for the  $A_1$  (LO) mode in  $c$ -plane InN epilayers. We attribute the quenching of the LO intensity to the fact that the UV excitation energy is far away from the electronic resonance conditions which greatly enhance the Raman intensities of the polar modes as the excitation wavelength approaches the red and infrared regions.<sup>7,13</sup> Thus, the electric-field induced Fröhlich resonance does not take place under UV excitation and the forbidden  $E_1$  (LO) scattering at the accumulation layer can no longer be observed. Within the core of the nanowires, the  $E_1$  (LO) mode is coupled with plasmons so only the  $L^-$  mode can be detected. This mode follows the same selection rules as the  $E_1$  (LO) mode,<sup>14</sup> and it is therefore dipole allowed for in-plane, off-backscattering geometry. A narrow  $E_1$  (TO) peak can also be distinctly observed, most notably in sample S3.

In order to estimate the volume electron density in the nanowires, we have fitted a dielectric line shape model to the  $L^-$  Raman spectra. The model involves linear response of the lattice-electron-gas system within the dissipation-fluctuation framework, in which the electron contribution is evaluated by means of the Lindhard–Mermin dielectric function. Details of the model and material parameters specific for InN can be found in Ref. 7. The model was applied to fit the visible ( $\lambda_{\text{exc}}=514.5$  nm) Raman spectra of a set of InN epilayers with electron densities ranging from  $2 \times 10^{18}$  to  $2 \times 10^{19}$   $\text{cm}^{-3}$  and a good agreement was found with the Hall data.<sup>7</sup> Although the UV spectra reveal more distinct peaks than the visible spectra, we have applied the model to the

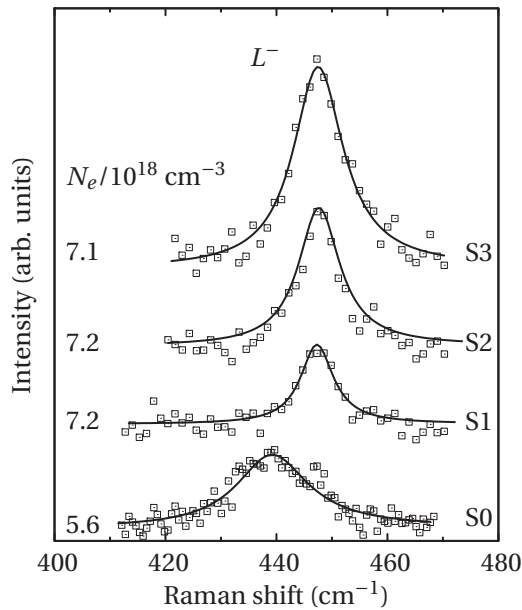


FIG. 3. Line shape fits (solid lines) to the visible Raman spectra of the  $L^-$  phonon-plasmon coupled mode (open squares) for the undoped InN nanowires (S0) and for the Si-doped nanowires (S1–S3). The Si background has been subtracted from the spectra.

latter to avoid the possible influence of the strong optical absorption on the electron density determination. It should be pointed out that in contrast with Ref. 7, where the coupling took place with the  $A_1$  (LO) mode, here we have used the  $E_1$  frequencies (determined from our own Raman measurements) to implement the phonon-plasmon coupling. Calculations are made in the assumption of isotropic conduction band and dielectric constant. Prior to the fits, the Si background has been carefully subtracted from the spectra. Figure 3 shows the  $L^-$  line shape fits (solid lines) to the visible Raman spectra (open squares) of the undoped and Si-doped nanowires. The fits yield an electron density of  $N_e = 5.6 \times 10^{18} \text{ cm}^{-3}$  for the undoped samples, which may be related to the defects and stacking faults present at the base of the nanowires, and may also indicate some degree of Si intermixing from the Si substrate. This electron density is in good agreement with previous estimations derived from the analysis of photoluminescence spectra.<sup>9</sup> A higher electron density is obtained for the Si doped samples ( $N_e \sim 7.2 \times 10^{18} \text{ cm}^{-3}$ ), although no significant differences in  $N_e$  can be found among the samples S1–S3 grown with different Si fluxes. This suggests that Si incorporation is not very large and rapidly saturates. For the Mg-doped samples, the  $L^-$  signal is too weak and broad to permit its unambiguous distinction from the Si second-order spectrum and the line shape fit was not attempted. However, from the downward frequency shift of the  $L^-$  peak revealed in the UV spectra [see Fig. 1(b)], we estimate an electron density of  $N_e \approx 4.6 \times 10^{18} \text{ cm}^{-3}$  in the Mg-doped samples. This indicates that a partial compensation of the  $n$ -type conductivity occurs in the Mg-doped samples, as previously reported in InN epilayers.<sup>15</sup>

As can be seen in Fig. 2, all nanowire samples display the same relaxed  $E_2^{\text{high}}$  frequency, indicating that the possible incorporation of impurities is not high enough to result into a measurable hydrostatic strain. The  $E_2^{\text{high}}$  full width at half maximum in the undoped sample ( $3.7 \text{ cm}^{-1}$ ) compares fa-

vorably to that of the best quality epitaxial layers measured by our group ( $5.1 \text{ cm}^{-1}$  at room temperature for sample A1 of Ref. 7). While Si doping appears to slightly degrade the crystal quality and/or the homogeneity of the nanowires, which leads to a broader  $E_2^{\text{high}}$  peak and to a higher intensity of the DALO band, the crystal quality of the nanowires is essentially unaffected by Mg doping. The DALO band observed in the Mg doped samples is probably related to the defects and stacking faults present at the base of the nanowires.

In summary, a Raman scattering investigation of undoped as well as Si-doped and Mg-doped InN nanowires has been performed. The most salient features of the visible and UV Raman spectra of the nanowires have been discussed in terms of scattering geometries and resonance mechanisms. The absence of the LO Raman peak in the out of resonance UV spectra supports the interpretation that the unscreened LO modes arise from electric-field induced forbidden scattering in the accumulation layer. An  $L^-$  LO-phonon-plasmon coupled mode has been observed that shifts to higher (lower) frequencies in Si- (Mg-) doped samples. A line shape analysis of the  $L^-$  Raman peak has allowed us to determine the electron density in the volume of the undoped nanowires which is found to be in the mid- $10^{18} \text{ cm}^{-3}$ . Only a moderate increase ( $\sim 30\%$ ) of the electron density is observed in the Si-doped samples, irrespective of the Si flux used during the growth. The electron density is reduced ( $\sim 18\%$ ) in Mg-doped samples, indicating that electrical activation of Mg occurs in Mg-doped nanowires.

This work has been supported by the Spanish Ministry of Science and Innovation under Contract No. MAT2007-63617.

- <sup>1</sup>R. W. Martin, P. R. Edwards, R. Pecharrroman-Gallego, C. Liu, C. J. Deatcher, I. M. Watson, and K. P. O'Donnell, *J. Phys. D* **35**, 604 (2002).
- <sup>2</sup>M. A. Sánchez-García, J. Grandal, E. Calleja, S. Lazic, J. M. Calleja, and A. Trampert, *Phys. Status Solidi B* **243**, 1490 (2006).
- <sup>3</sup>Y.-L. Chang, Z. Mi, and F. Li, *Adv. Funct. Mater.* **20** (2010).
- <sup>4</sup>L. Hsu and W. Walukiewicz, *J. Appl. Phys.* **104**, 024507 (2008).
- <sup>5</sup>L. Colakerol, T. D. Veal, H.-K. Jeong, L. Plucinski, A. DeMasi, T. Learmonth, P.-A. Glans, S. Wang, Y. Zhang, L. F. J. Piper, P. H. Jefferson, A. Fedorov, T.-C. Chen, T. D. Moustakas, C. F. McConville, and K. E. Smith, *Phys. Rev. Lett.* **97**, 237601 (2006).
- <sup>6</sup>C. G. Van de Walle and D. Segev, *J. Appl. Phys.* **101**, 081704 (2007).
- <sup>7</sup>R. Cuscó, J. Ibáñez, E. Alarcón-Lladó, L. Artús, T. Yamaguchi, and Y. Nanishi, *Phys. Rev. B* **79**, 155210 (2009).
- <sup>8</sup>R. Cuscó, E. Alarcón-Lladó, J. Ibáñez, T. Yamaguchi, Y. Nanishi, and L. Artús, *J. Phys.: Condens. Matter* **21**, 415801 (2009).
- <sup>9</sup>T. Stoica, R. J. Meijers, R. Calarco, T. Richter, E. Sutter, and H. Lüth, *Nano Lett.* **6**, 1541 (2006).
- <sup>10</sup>E. O. Schäfer-Nolte, T. Stoica, T. Gotschke, F. A. Limbach, E. Sutter, P. Sutter, D. Grützmacher, and R. Calarco, *Nanotechnology* **21**, 315702 (2010).
- <sup>11</sup>E. Alarcón-Lladó, J. Ibáñez, R. Cuscó, L. Artús, J. D. Prades, S. Estradé, and J. R. Morante, "Ultraviolet Raman scattering in ZnO nanowires: Quasimode mixing and temperature effects," *J. Raman Spectrosc.* (in press).
- <sup>12</sup>E. Calleja, J. Grandal, M. A. Sánchez-García, M. Niebelschütz, V. Ci-malla, and O. Ambacher, *Appl. Phys. Lett.* **90**, 262110 (2007).
- <sup>13</sup>M. Kuball, J. W. Pomeroy, M. Wintrebert-Fouquet, K. S. A. Butcher, H. Lu, W. J. Schaff, T. V. Shubina, S. V. Ivanov, A. Vasson, and J. Leymarie, *Phys. Status Solidi A* **202**, 763 (2005).
- <sup>14</sup>*Light Scattering in Solids*, edited by M. Cardona (Springer, Berlin, 1975), Vol. 1.
- <sup>15</sup>V. Y. Davydov, V. V. Emtsev, I. N. Goncharuk, A. N. Smirnov, V. D. Petrikov, V. V. Mamutin, V. A. Vekshin, S. V. Ivanov, M. B. Smirnov, and T. Inushima, *Appl. Phys. Lett.* **75**, 3297 (1999).